PAUL SCHERRER INSTITUT

SWISS LIGHT SOURCE SLS

SLS-TME-TA-2003-0222
21st January 2003

SLS-FEMTO: Beam halo formation and maximum repetition rate for laser slicing

Andreas Streun

Paul Scherrer Institut, CH-5232 Villigen PSI, Switzerland

1 Introduction

The SLS-FEMTO insertion will produce sub-picosecond X-ray pulses by laser induced energy modulations of very short electron beam slices in a wiggler (the “modulator”). Variation of dispersion translates the energy modulations into horizontal angles in an undulator downstream (the “radiator”). There, the radiation from the beam slices (the “satellites”) separates from the much stronger core beam radiation and thus can be extracted by a simple blade at some distance down the photon beamline.

The satellites survive laser interactions and will be captured by the storage ring acceptance, which of course is intended, otherwise the beam life time would become as short as one second (= inverse product of laser repetition frequency and slicing efficiency).

The satellites perform betatron oscillations around the core beam. Within a few hundred turns they will completely filament transversely due to chromatic and amplitude dependant tune shifts and form a homogeneous beam halo. The halo will slowly shrink and merge back into the core beam due to radiation damping at a time constant of about 8 ms in case of SLS with FEMTO at 2.4 GeV.

With proposed laser repetition frequencies of $1 \ldots 10$ kHz a halo will accumulate over several interactions. The background from the halo thus could become stronger than the desired signal from the fresh interaction and seriously disturb the experiment.

Since pushing for high repetion frequency increases dramatically the costs of the laser system, it was necessary to investigate whether a large frequency can be really exploited, considering the background signal from the FEMTO-halo.

This paper continues previous work on the halo problem as documented in [1] and sec.6 of [2], and is based on the chicane layout for large horizontal separation as documented in [3].

2 Analytical estimate

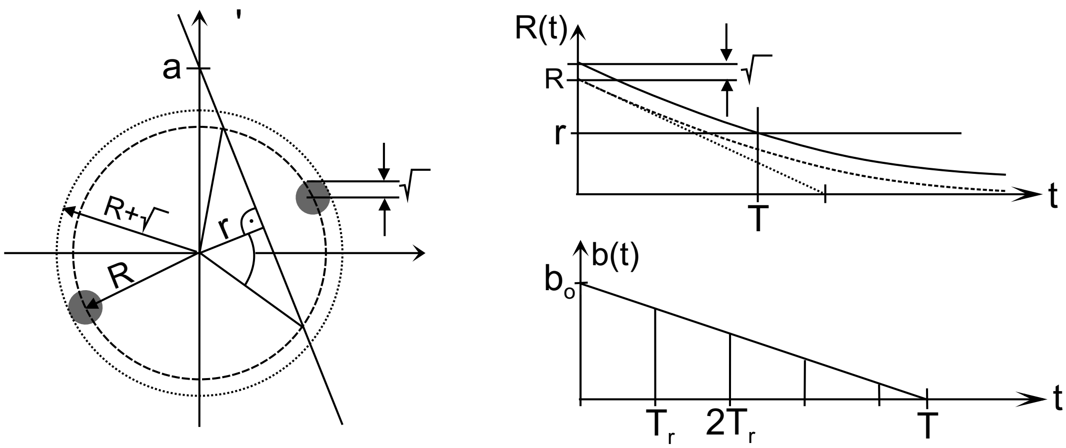

Figure 1: Simplified model for estimation of halo background

left: In normalized horizontal phase space, the betatron oscillation moves the satellite beams on a circle of radius R and forms a halo due to filamentation. The blade in front of the experiment appears at a slanted line. Halo regions which are right of this line will create a signal at the experiment. When the halo shrinks to hide behind the blade due to radiation damping, the signal will disappear.

right/top: Approximation for the decay of the background signal and definition of halo decay time T. See text for further explanations.

right/bootom: Accumulation of background signal from sampling the halo signal over several repetitions of laser slicing.

In the angular separation scheme, the light from the radiator propagates a distance D to a blade blocking the core beam and the positive satellite, allowing only the light of the negative satellite to pass.

The blade in horizontal phase space appears at a line parallel to the x' axis with distance B to the origin and thus can be parameterized as $\vec{x} = (B, \lambda)$, $\lambda \in \mathcal{R}$.

Backtransformation to the radiator center and to normalized coordinates (χ, χ') using the local beam parameters gives another parameterization of the blade, shown as slanted line in fig.1(left):

$$\begin{pmatrix} \mu \\ a + m\mu \end{pmatrix} = \begin{pmatrix} \frac{1}{\sqrt{\beta}} & 0 \\ \frac{\alpha}{\sqrt{\beta}} & \sqrt{\beta} \end{pmatrix} \cdot \begin{pmatrix} 1 & -D \\ 0 & 1 \end{pmatrix} \cdot \begin{pmatrix} B \\ \lambda \end{pmatrix}$$

$$\text{with} \qquad \mu = \frac{B - \lambda D}{\sqrt{\beta}} \in \mathcal{R} \qquad a = \frac{\sqrt{\beta}B}{D} \qquad m = \alpha - \frac{\beta}{D}$$

In normalized phase space, the beam ellipse describing the electron ensemble appears as circle of radius $\sqrt{\varepsilon}$. The satellite beams also appear as circles of same size located on a major circle given by the betatron amplitude induced by the energy variation δ due to laser interaction: The large circle's radius is given by

$$R = \sqrt{H}\,\delta,$$

where H is the dispersion's emittance created by the modulator chicane [2]. With each turn the satellites rotate by an angle of $2\pi\nu$ counterclockwise on the major circle, where ν is horizontal tune of the machine.

For background estimate we have to consider different time scales:

- In the next turns after interaction there will be a strong but fluctuating background signal, depending on if one of the satellites appears in the right region of fig.1(left) above the blade or not.
- After a few hundred turns the satellite beams will filament transversely and cover the complete circumference of the large ring homogeneous in angle, i.e. a halo has formed. Thus the background signal will be of constant intensity and given by the opening angle 2ϕ in fig.1(left).
- Within a few thousand turns the halo will shrink due to radiation damping. When all of the halo is under the blade, the background signal will disappear.

To estimate the average *initial* background signal b_o we are allowed to assume $\sqrt{\varepsilon} \ll R$ and thus may simply compare the "visible" arc of angle 2ϕ with the full circumference and multiply it by 2, since we have two satellites rotating:

$$b_o = 2\,\frac{2\phi}{2\pi} \quad \text{with} \quad \phi = \arccos\frac{r}{R},$$

where r is the minimum distance of the backtransformed blade to the origin, see fig.1(left), and given by

$$r = \frac{a}{\sqrt{1+m^2}}.$$

The initial radius enclosing what is becoming the beam halo is approximately given by $R + \sqrt{\varepsilon}$. This radius shrinks due to radiation damping approaching a final value of $\sqrt{\varepsilon}$ to merge into the core beam. Thus, if the blade is sufficiently far away from the origin ($r > \sqrt{\varepsilon}$, which of course is required to block the core beam), the background signal will disappear at a time T, when the shrinking halo radius reaches r, see fig.1(right/top). With τ the horizontal radiation damping time, we thus get an estimate for the halo decay time T by

$$r = R\,e^{-T/\tau} + \sqrt{\varepsilon} \qquad \Longrightarrow \qquad T = -\tau \ln\frac{r-\sqrt{\varepsilon}}{R}$$

The background signal does not follow a pure exponential law, since the accepted angle 2ϕ closes like a pair of scissors during damping. The exact function of background on time could be calculated (by integration of the ring shaped gaussian distribution accepted by the blade as function of time), but for our estimate it is sufficient to approximate it by a simple linear slope as shown in fig.1(right/bottom):

$$b(t) = b_o \left(1 - \frac{t}{T}\right)$$

If the repetiotion time of the laser $T_r = 1/f_r$ is smaller than T, background from one or more previous pulses will disturb the signal. Defining

$$n = \frac{T}{T_r}$$

the total background is given by ($[n]$ means the largest integer $< n$)

$$b = \sum_{k}^{[n]} b_o \left(1 - k\frac{T_r}{T}\right) = b_o[n] \left(1 - \frac{[n]+1}{2n}\right) \quad \xrightarrow{n \gg 1} \quad b \approx \frac{b_o T}{2} f_r$$

If the repetition time T_r is much shorter than the halo decay time T, the background is given by the triangle area in fig.1(right/bottom), repeated with the frequency f_r.

Now we insert the following parameters into the formulae:

Horizontal distance of blade from origin	B	7 mm
Longitudinal distance of blade from radiator center	D	15 m
Horizontal betafunction at radiator center	β	8.81 m
Horizontal alphafunction at radiator center	α	-2.17
Dispersions emittance from modulator chicane	H	0.0186 m·rad
Relative energy change due to laser interaction	δ	$\pm 5.4 \cdot 10^{-3}$
Ring emittance (incl. modulator contribution [3])	ε	7.2 nm·rad
Ring horizontal damping time (incl. modulator)	τ	8.1 ms
$\Longrightarrow$ Initial average background signal (relative)	b_o	**0.56**
$\Longrightarrow$ Halo decay time	T	**5.2 ms**

Following table gives the total background (normalized to the signal at laser interaction) as a function of the laser repetition rate:

Repetition rate	f_r	≤192 Hz	250 Hz	500 Hz	1 kHz	5 kHz
Total background signal	b	0	0.13	0.47	1.18	7.0

If a number of M electron bunches alternatingly is used for pulse slicing, and if a shutter with rise/fall times of $< 480/M$ ns exists (960 ns is the ring revolution frequency), the maximum repetion rate to avoid any halo background can be increased to $M \cdot 192$ Hz.

Previous studies of the halo problem had alreay proven, that there will be no background in multi-bunch mode, however this would require a 1 ns on/off gating of the experiment [1].

3 Tracking studies

The above estimates had to be confirmed by a tracking study using the TRACY code. Furthermore, the spectral distribution of the background had to be investigated, considering an experiment which would be sensitive only to a short pulse time structure.

3.1 Modelling

An ensemble of 2000 particles $\{\vec{r}_i\}$ with 6-dimensional Gaussian distributions and standard deviations of 1 was generated. Physical coordinates were set by the following transformations:

$$\begin{pmatrix} \frac{\Delta p}{p} \\ \Delta s \end{pmatrix} = \begin{pmatrix} \sigma_e & 0 \\ 0 & c\,\sigma_t \end{pmatrix} \begin{pmatrix} r_5 \\ r_6 \end{pmatrix} \qquad \begin{pmatrix} y \\ p_y \end{pmatrix} = \begin{pmatrix} 0 \\ 0 \end{pmatrix}$$

$$\begin{pmatrix} x \\ p_x \end{pmatrix} = \begin{pmatrix} \sqrt{\beta}_{xm} & 0 \\ -\frac{\alpha_{xm}}{\sqrt{\beta_{xm}}} & \frac{1}{\sqrt{\beta_{xm}}} \end{pmatrix} \sqrt{\varepsilon_x} \begin{pmatrix} r_1 \\ r_2 \end{pmatrix} + \begin{pmatrix} \eta_{xm} \\ \eta'_{xm} \end{pmatrix} \frac{\Delta p}{p}$$

The subscript $_m$ indicates that the beam parameters are to be taken at the *modulator* center. The vertical coordinates were set to zero since the calculations were done for an ideal SLS-lattice where there is neither emittance nor dispersion in the vertical. Since the synchrotron tune is rather low, correlations between energy and longitudinal position were neglected and only one ideal cavity providing 2.6 MV of accelerating voltage was assumed. σ_e is the natural energy spread, σ_t is the rms laser pulse duration and was set to $\sigma_t = 50$ fs.

Each 1000 particles were shifted in energy by $\delta = \pm 5.4 \cdot 10^{-3}$ to simulate the energy change due to laser interaction. This is an idealized model, since the laser modulation is not a clean rectangular pulse but rather a Gaussian peak, with modulations ranging between 0 and the full value.

The optics mode D2R was set for the lattice, it provides betatron tunes of 20.38/8.16 which are shifted by the FEMTO-insertion to 20.38/8.66.

Here are the lattices equilibrium data as calculated by TRACY: (4^{th} order symplectic integrator, 4 kicks per quadrupole, 5 per bend, 2 per wiggler pole):

Machine tunes	ν_x, ν_y, ν_s	20.376, 8.659 , 0.007047
Chromaticities	ξ_x, ξ_y	0.99, 0.95
Emittances	ε_x, ε_y	6.76 nm, 0
Energy spread and bunchlength (rms)	σ_e, σ_s	8.72·10^{-4}, 3.45 mm
Momentum compaction factor	α	6.1444·10^{-4}

TRACY's results depend on the number of kicks per element when using the symplectic integrator for complete modelling, and therefore the emittance is too low by 6 % for the settings chosen, compromising running time vs. precision. However this small discrepancy has little impact on the result.

The particles were tracked for 5000 turns. At selected turns the 6-dimensional particle data taken at the center of the radiator were written to files for postprocessing.

3.2 Evaluation

Each [macro]particle arriving at the radiator centre is treated as the origin of a [macro] photon. The photons are propagated by the distance $D = 15$ m to the blade and filtered. Histograms for spatial and temporal distributions are calculated.

In order to give an estimate of the spectral distribution, the evaluation proceeds by the following steps:

1. The temporal histogram corresponds to light intensity for incoherent superposition, as it is adequate for an experiment operating in the X-ray regime. Note: when working in the IR-regime as the diagnostics beamline X05DB will do, coherent superposition would, have to be considered!

2. The intensity histogram with values h_k ($k = 1 \ldots N$) and width Δt corresponds to integrated squared field strenghts, thus a time signal is reconstructed by

$$a(t_k) = \sqrt{\frac{h_k}{\Delta t}}$$

   No phase information is available, however the frequencies we consider (X-ray!) are large compared to Δt, thus the phase varies fast anyway.

3. A frequency spectrum is obtained from a Fourier transform of the time signal with a corresponding frequency space $\{f_n\}$:

$$A_n = \frac{1}{N} \sum_{k=0}^{N-1} a_k e^{2\pi i k n/N}, \quad f_n = \frac{n}{N\Delta t}, \quad n = -\frac{N}{2}, \ldots, 0, \ldots, \frac{N}{2}$$

4. The one-sided power spectrum is calculated by

$$P_n = |A_n|^2 + |A_{-n}|^2 \qquad n = 0 \ldots N/2$$

   and integrated from some frequency to infinity (i.e. the Nyquist frequency) to summarize high frequency contributions, and normalized to come back to physical units:

$$I(f) = \int_f^\infty P(f')\, df' \quad \longrightarrow \quad I(f_m) = \frac{\Delta t}{N} \sum_{n=m}^{N/2} P_n$$

   Of course the total integral equals the number of [macro] photons in the histogram: $I(0) = \sum h_k$ (Parseval's theorem).

3.3 Results

The figures at the end of this paper show snapshots from a few turns:

Turn 0: Immediately after laser interaction in the modulator, the satellite with negative energy offset appears right of the transformed blade and thus sends light to the experiment. In longitudinal phase space, a sharp line appears corresponding to the short pulse. The temporal structure however shows that the slice has widened from the original 50 fs (rms) to 77 fs which is due to the third chicane magnet. The spectrum extends to rather high frequencies as it is desired in this first shot.

Turn 1: One turn later the two satellites have almost changed their locations due to betatron oscillations. The same intensity arrives at the experiment, but the high frequency component is reduced, since the synchrotron phase advance for one turn lengthens the satellite bunches to 0.5 ps rms.

Turn 35: After 1/4 synchrotron oscillation the energy distribution has been rotated onto the time axis, thus the natural bunch length σ_s/c = 3.45 mm/c = 11.5 ps appears in the temporal distribution and histogram and the spectrum is cut off already around 20 GHz.

Turn 143: Each n/2 synchrotron oscillations the short pulse recoheres and with it the high freqency background as shown here after the first period ($n = 2$). Filamentation of betatron motion is already in progress and will be complete after approx. 300 turns, whereas the synchrotron motion is well correlated except a beginning propeller-shaped distortion.

Turn 998: A halo has developed and slowly shrinks due to radiation damping. The background at the experiment is still approx. 50 % of the initial signal and high frequency components appear every half synchrotron period. The time signal shows more than one peak since radiation comes from the remains of both satellites.

Turn 4044: Radiation damping shrinks the halo to hide behind the blade and the background slowly disappears. After 5000 turns the background is less than 2 %. Eventually, filamentation of the synchrotron motion becomes appearent.

Figure 2 shows the background signal in the three frequency domains: The high frequency contribution decoheres quickly but recoheres at the double synchrotron tune $2\,\nu_s$. The total background is wildly fluctuating on the first few hundreds turns due to betatron oscillations and becomes smooth due to filamentation as visible figure in the upper right window of the figure.

A linear fit to the total background, shown as dotted line in figure 2 (bottom), gave for initial background signal and halo decay time:

$$\mathbf{b_o = 0.587} \qquad \mathbf{T} = 4.8 \text{ ms}$$

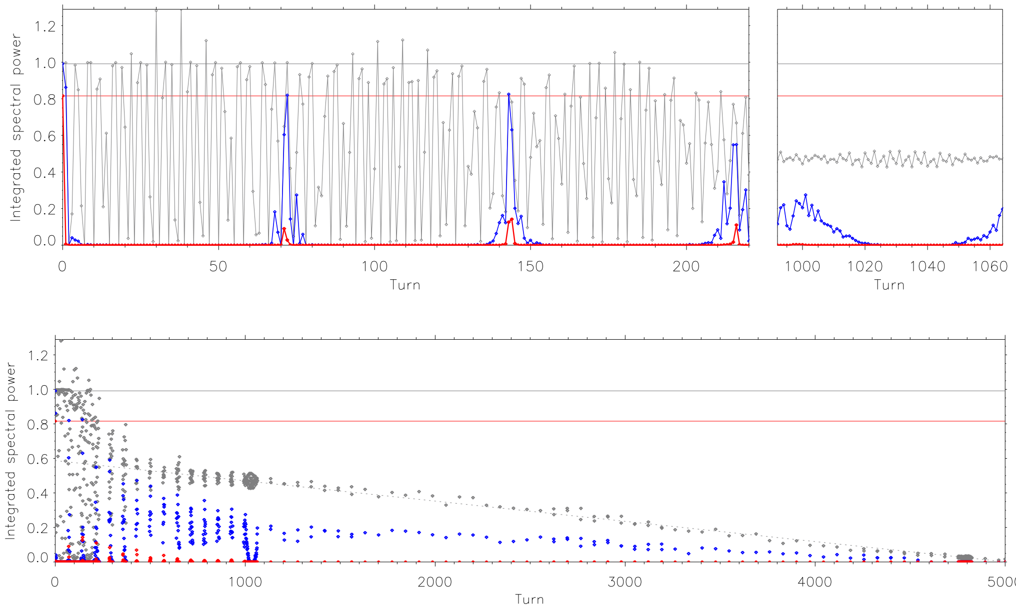

Figure 2: Background signal as a function of turn number

Total signal (grey), above 100 GHz (blue) and above 500 GHz (red). A value of 1.0 corresponds to the intensity from one full satellite beam or 1000 particles. The red horizontal line marks the [desired] high frequency signal from the first interaction.

Top: Magnified windows of interesting regions

Bottom: All data, not all turns shown. The dotted line is a linear fit to the total background

which agrees very well with the analytical estimate. Consequently, the integrated background intensities for various repetition rates confirm the data given above:

Repetition rate	f_r	$\leq$208 Hz	250 Hz	500 Hz	1 kHz	5 kHz
Total background signal	b	0	0.10	0.44	1.1	6.7

The high frequency background (>500 GHz) decays much faster. After 0.3 ms it is at $\approx$ 10 % of its initial value, after 1 ms less than 1 %. Thus if the experiment is not sensitive to low frequency noise, a higher repetition rate may be feasible.

4 Conclusions

An analytic formula derived for the background signal from the beam halo agrees very well with tracking simulations and thus may be used for further estimates.

With present parameters, the repetition rate for beam laser interaction must not be higher than 200 Hz in order to avoid any background signal from previous laser interactions.

At a repetition rate of 1 kHz as originally proposed, the signal to noise ratio is below 1, i.e. the background is stronger than the desired signal.

If the experiment is sensitive to high frequency noise only, a higher repetition rate may be feasible. Tolerating noise above 500 GHz of up to 1 % of the initial signal would allow 1 kHz repetition.

Alternating interactions with M bunches in the ring allow to increase the maximum repetition rate to M-times its beforementioned value, provided that very fast shutters or gates with rise and fall times below $< 480/M$ ns are available to block halo radiation from the other bunches.

References

[1] G. Singh, FEMTO – preliminary studies of effects of background electron pulses, SLS-TME-TA-2001-0180

[2] A. Streun, Some considerations on the SLS FEMTO insertion, SLS-TME-TA-2002-0199

[3] A. Streun, SLS-FEMTO: Chicane layout, performance and side-effects, SLS-TME-TA-2003-0223

Explanation of the figures on the following pages:

The figures show snapshots of particle distributions and spectra for some interesting turns after beam laser interaction:

- Upper right: Normalized horizontal phase space at radiator center. The backtransformed blade appears as dashed line, all particles right from it are transmitted – compare to figure 1 (left). Particle color corresponds to energy.

- Upper left: Longitudinal phase space and turn number.

- Middle left: Spatial distribution at the location of the blade, transmitted fraction shown red.

- Middle right: Temporal distribution, transmitted fraction shown red. The blue line is a Gauss fit to its most prominent peak. The number `ntt` is the intensity of the transmitted part, where 100 % corresponds to one full satellite, i.e. 1000 particles, and `stt` is the standard deviation of the distribution. `spk` is the sigma of the Gauss fit for comparison and `fpk` is the area under the blue Gaussian.

- Lower left: Power spectrum with two vertical lines corresponding to cut-offs at 100 GHz and 500 GHz. Of course, some high frequency noise appears due to bad statistics when sorting the particles into the histogram bins (the bin size corresponds to the Nyquist frequency).

- Lower right: Integrated power spectrum with numbers given for the integrals I(0), I(100 GHz) and I(500 GHz). I(0) of course equals the number of transmitted particles.

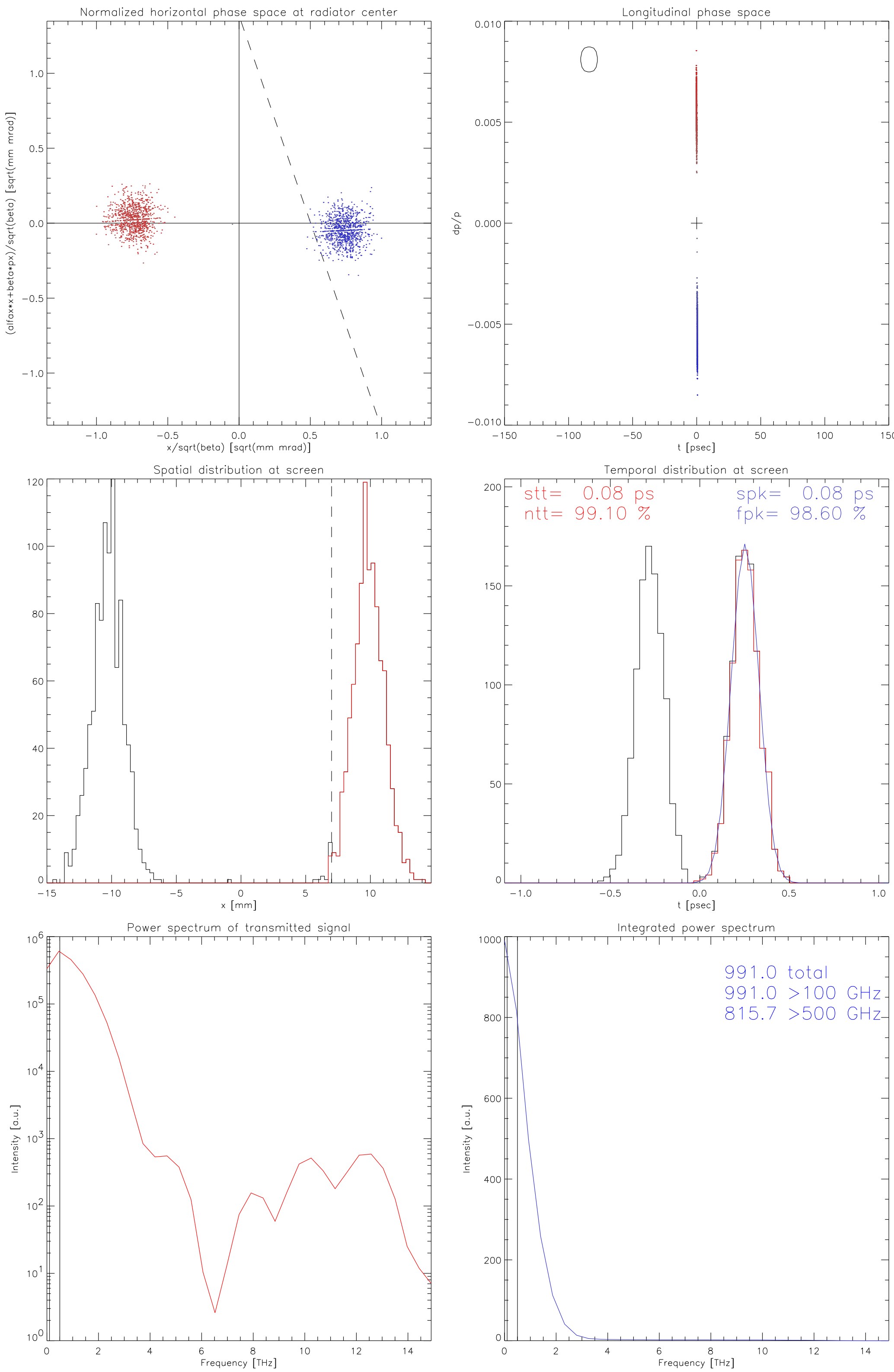
Normalized horizontal phase space at radiator center
(alfax*x+beta*px)/sqrt(beta) [sqrt(mm mrad)]
x/sqrt(beta) [sqrt(mm mrad)]
Longitudinal phase space
dp/p
t [psec]
Spatial distribution at screen
x [mm]
Temporal distribution at screen
stt= 0.08 ps
ntt= 99.10 %
spk= 0.08 ps
fpk= 98.60 %
t [psec]
Power spectrum of transmitted signal
Intensity [a.u.]
Frequency [THz]
Integrated power spectrum
991.0 total
991.0 >100 GHz
815.7 >500 GHz
Intensity [a.u.]
Frequency [THz]

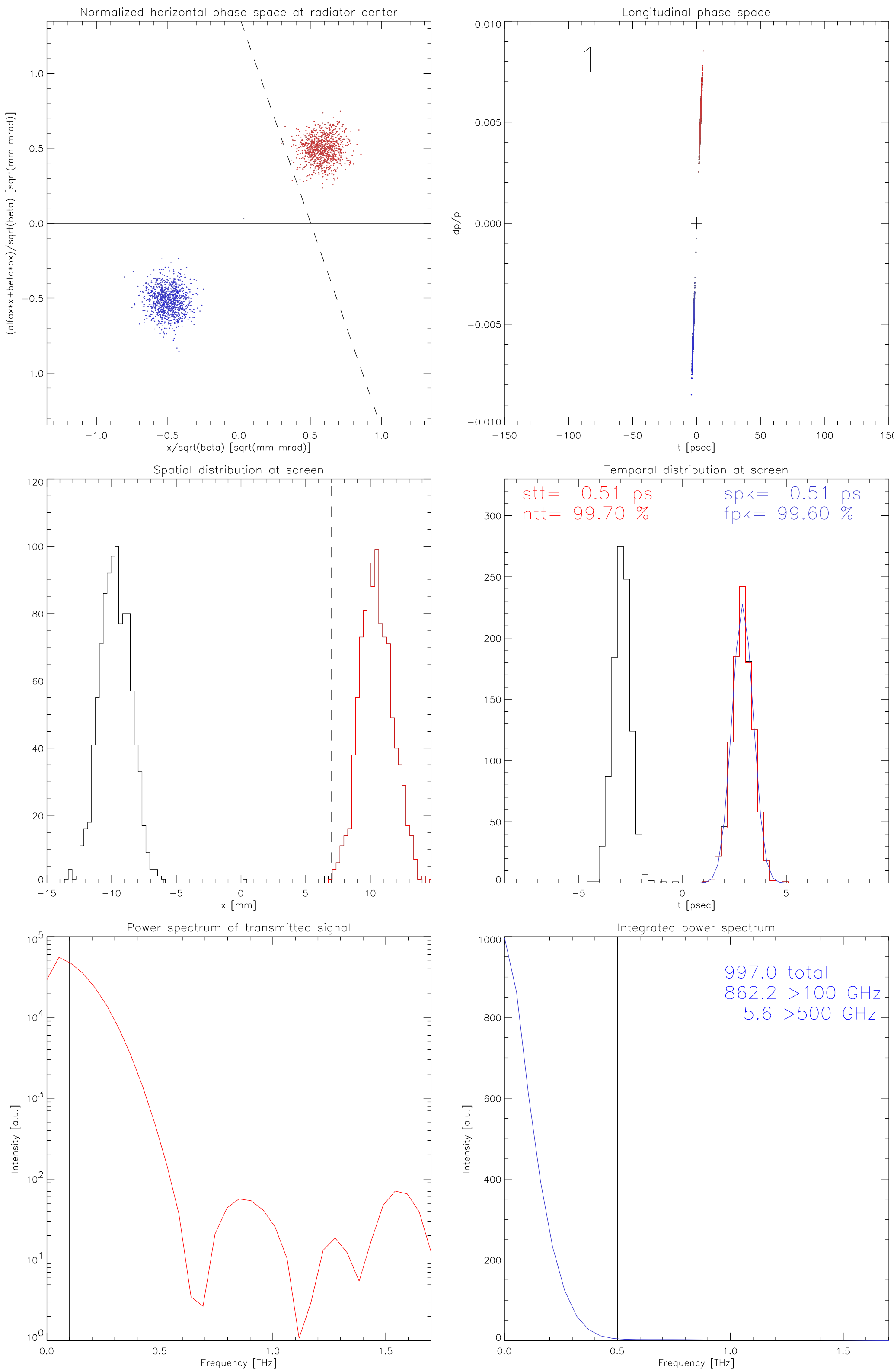
Normalized horizontal phase space at radiator center
(alfax*x+beta*px)/sqrt(beta) [sqrt(mm mrad)]
x/sqrt(beta) [sqrt(mm mrad)]
Longitudinal phase space
dp/p
t [psec]
Spatial distribution at screen
x [mm]
Temporal distribution at screen
stt= 0.51 ps
ntt= 99.70 %
spk= 0.51 ps
fpk= 99.60 %
t [psec]
Power spectrum of transmitted signal
Intensity [a.u.]
Frequency [THz]
Integrated power spectrum
997.0 total
862.2 >100 GHz
5.6 >500 GHz
Intensity [a.u.]
Frequency [THz]

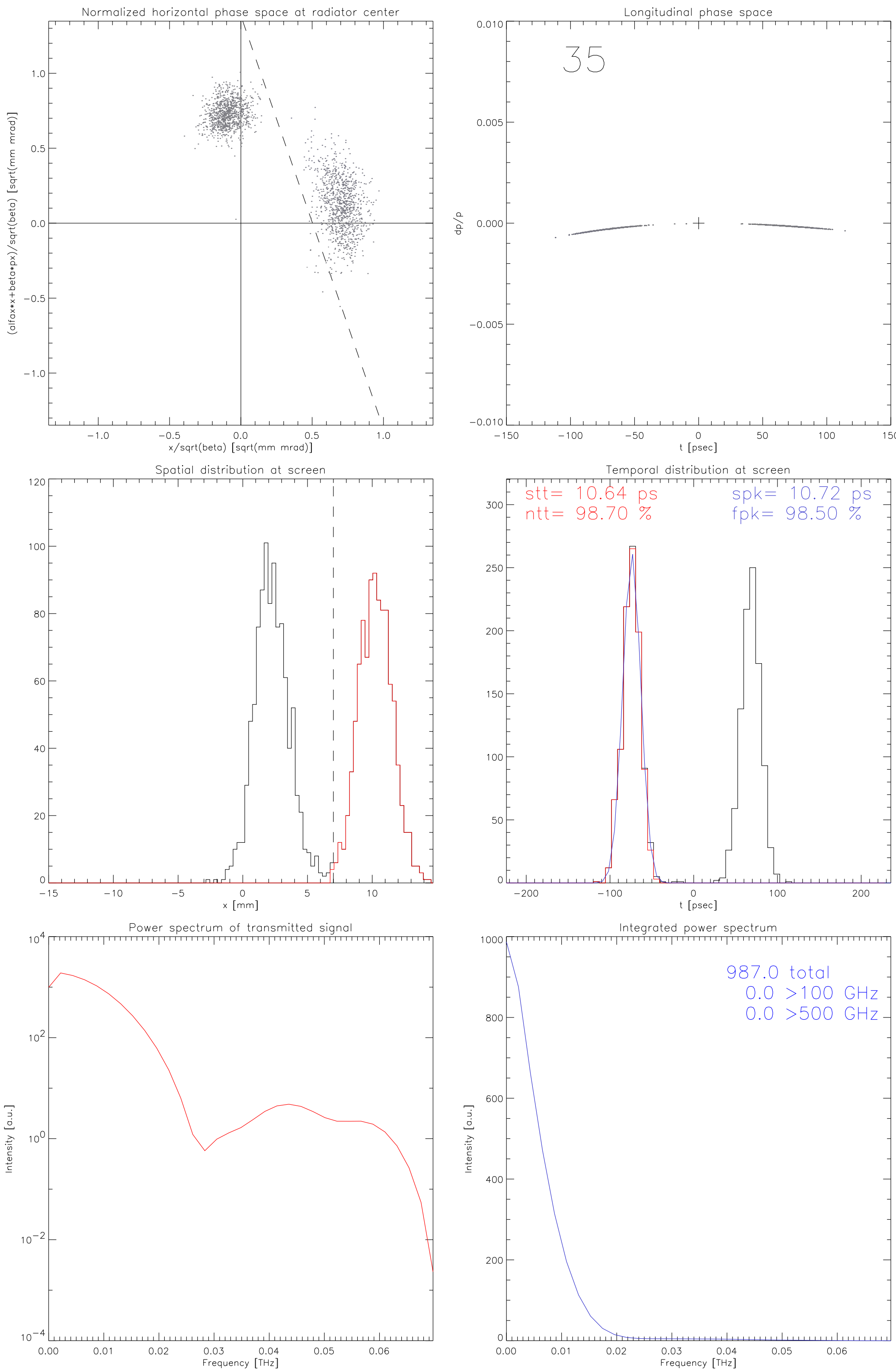
Normalized horizontal phase space at radiator center
(alfax*x+beta*px)/sqrt(beta) [sqrt(mm mrad)]
x/sqrt(beta) [sqrt(mm mrad)]
Longitudinal phase space
35
dp/p
t [psec]
Spatial distribution at screen
x [mm]
Temporal distribution at screen
stt= 10.64 ps
ntt= 98.70 %
spk= 10.72 ps
fpk= 98.50 %
t [psec]
Power spectrum of transmitted signal
Intensity [a.u.]
Frequency [THz]
Integrated power spectrum
987.0 total
0.0 >100 GHz
0.0 >500 GHz
Intensity [a.u.]
Frequency [THz]

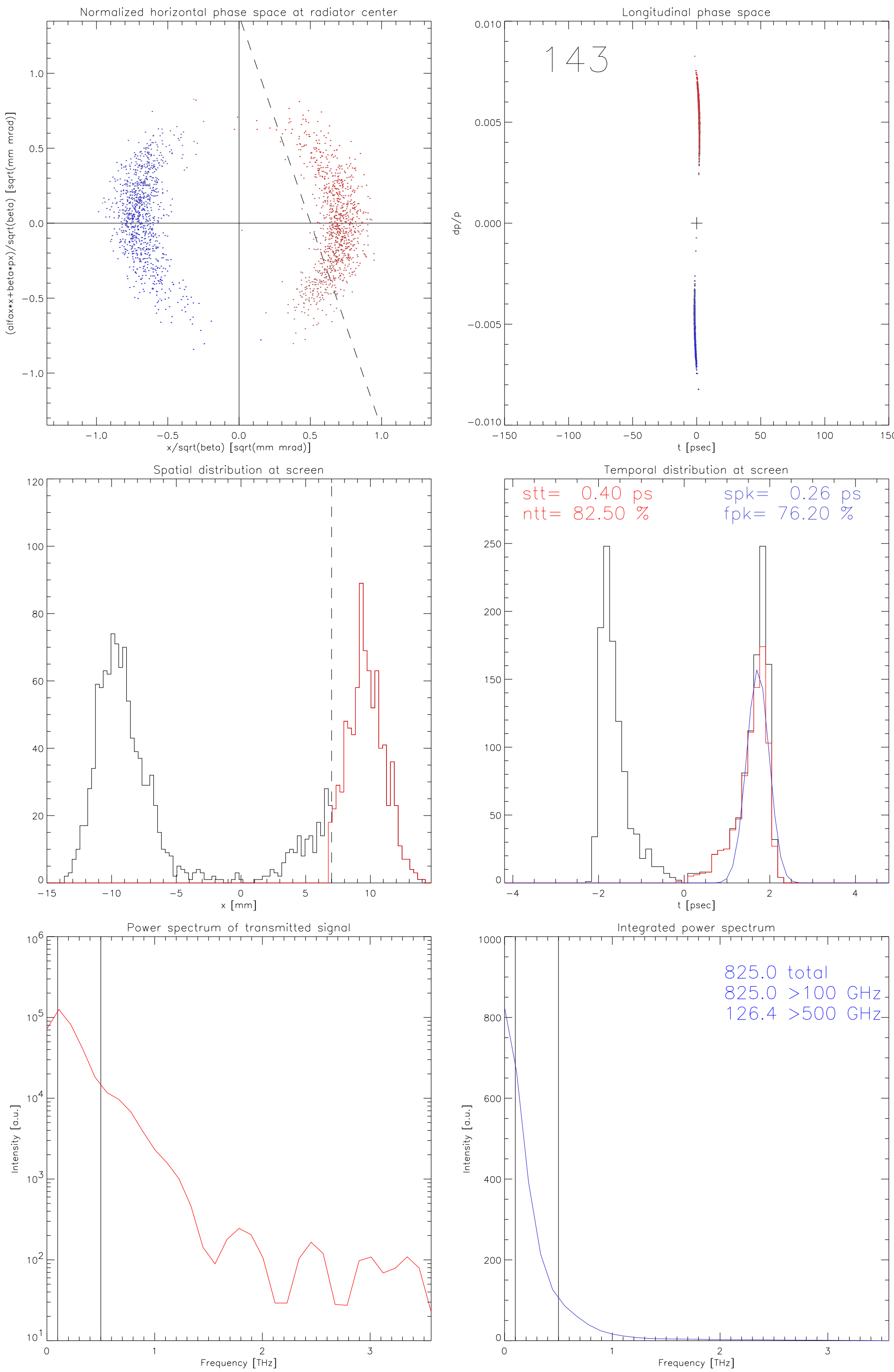
Normalized horizontal phase space at radiator center
(alfax*x+beta*px)/sqrt(beta) [sqrt(mm mrad)]
x/sqrt(beta) [sqrt(mm mrad)]
Longitudinal phase space
143
dp/p
t [psec]
Spatial distribution at screen
x [mm]
Temporal distribution at screen
stt= 0.40 ps
ntt= 82.50 %
spk= 0.26 ps
fpk= 76.20 %
t [psec]
Power spectrum of transmitted signal
Intensity [a.u.]
Frequency [THz]
Integrated power spectrum
825.0 total
825.0 >100 GHz
126.4 >500 GHz
Intensity [a.u.]
Frequency [THz]

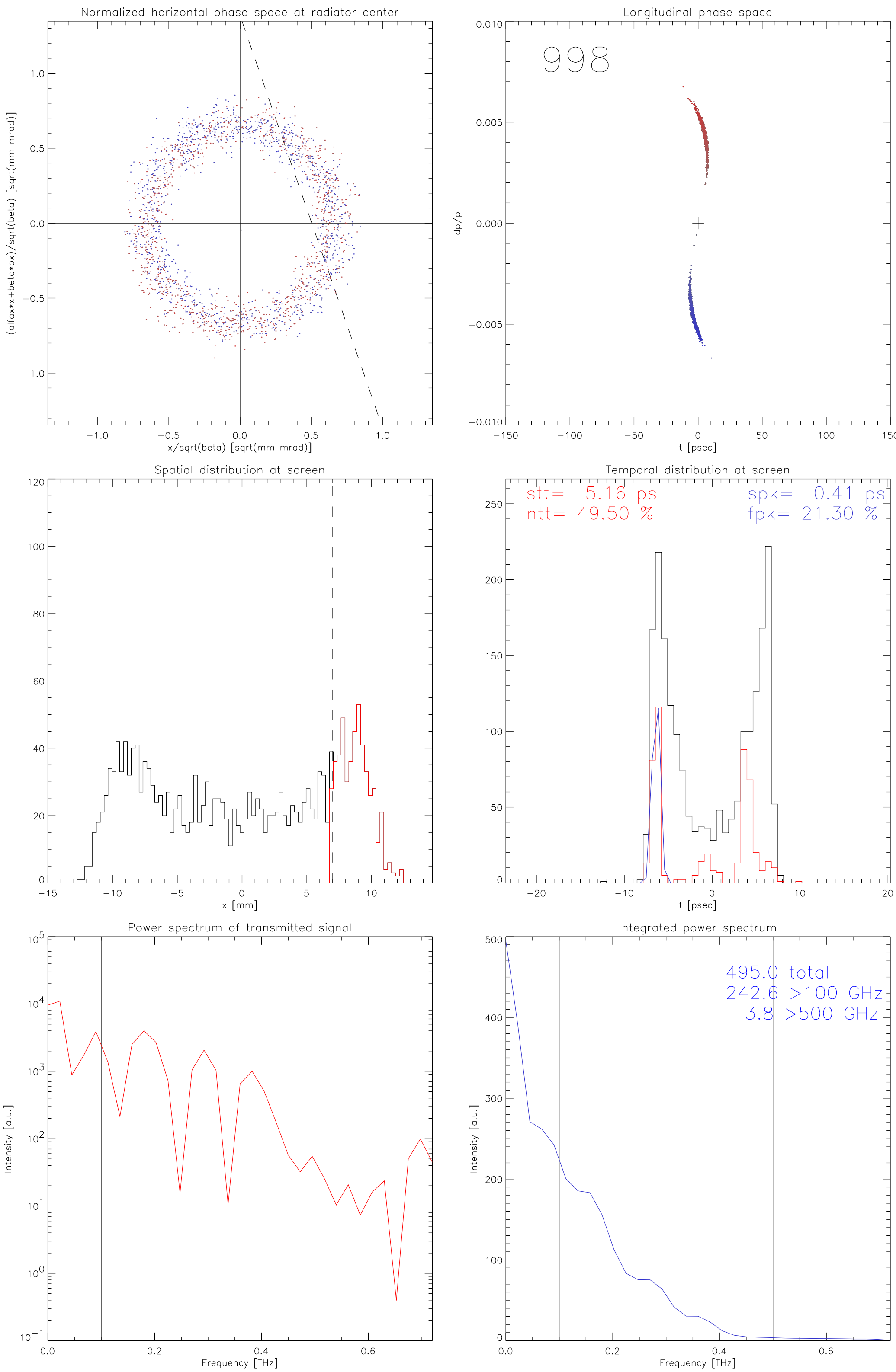
Normalized horizontal phase space at radiator center
(alfax*x+beta*px)/sqrt(beta) [sqrt(mm mrad)]
x/sqrt(beta) [sqrt(mm mrad)]
Longitudinal phase space
998
dp/p
t [psec]
Spatial distribution at screen
x [mm]
Temporal distribution at screen
stt= 5.16 ps
ntt= 49.50 %
spk= 0.41 ps
fpk= 21.30 %
t [psec]
Power spectrum of transmitted signal
Intensity [a.u.]
Frequency [THz]
Integrated power spectrum
495.0 total
242.6 >100 GHz
3.8 >500 GHz
Intensity [a.u.]
Frequency [THz]

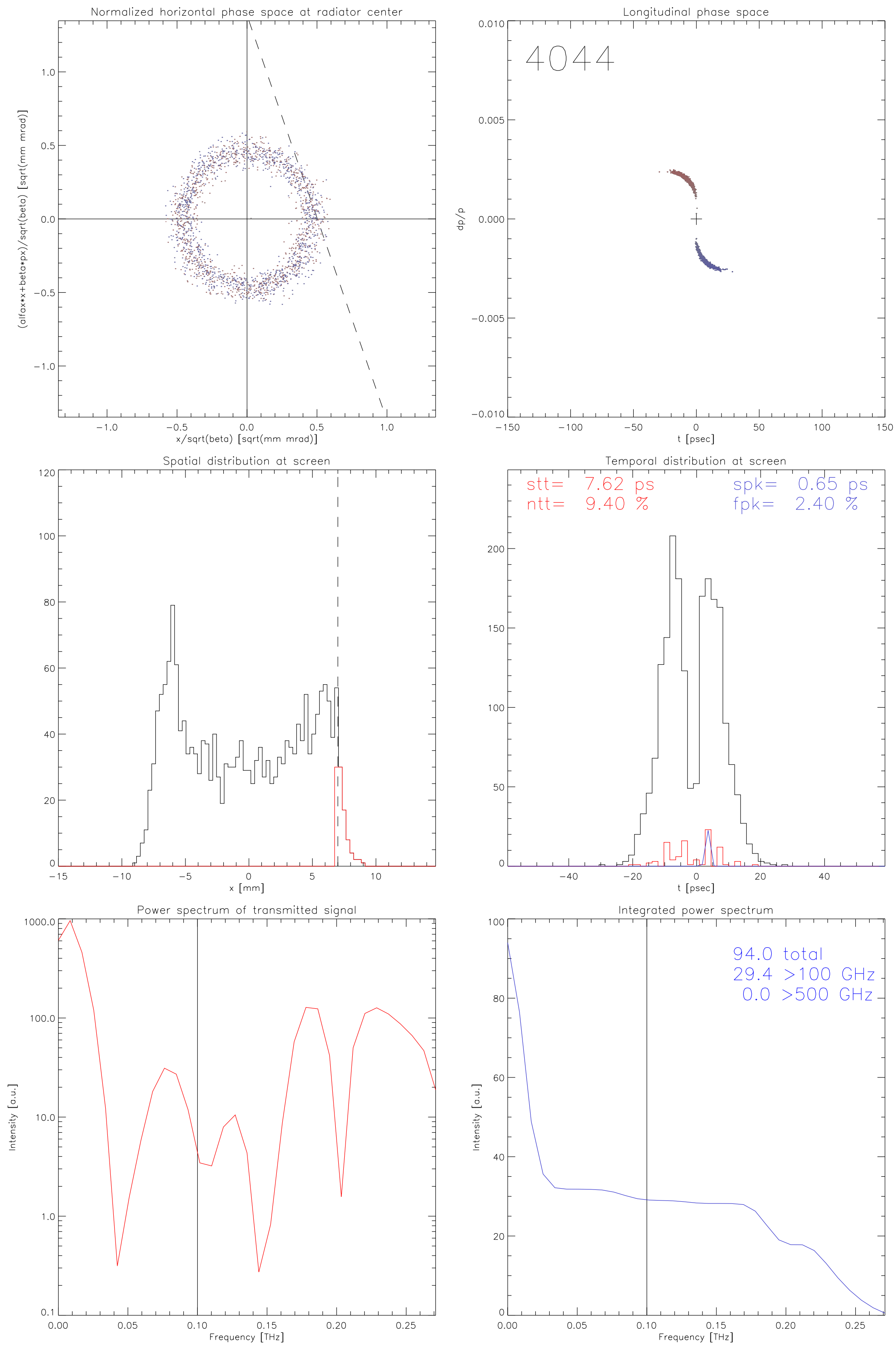
Normalized horizontal phase space at radiator center
(alfax*x+beta*px)/sqrt(beta) [sqrt(mm mrad)]
x/sqrt(beta) [sqrt(mm mrad)]
Longitudinal phase space
4044
dp/p
t [psec]
Spatial distribution at screen
x [mm]
Temporal distribution at screen
stt= 7.62 ps
ntt= 9.40 %
spk= 0.65 ps
fpk= 2.40 %
t [psec]
Power spectrum of transmitted signal
Intensity [a.u.]
Frequency [THz]
Integrated power spectrum
94.0 total
29.4 >100 GHz
0.0 >500 GHz
Intensity [a.u.]
Frequency [THz]